Novel erythropoietin-based therapeutic candidates with extra N-glycan sites that block hematopoiesis but preserve neuroplasticity

Milagros Bürgi[1], Gabriela Inés Aparicio[2], Aquiles Dorella[3], Ricardo Kratje[1], Camila Scorticati[2], Marcos Oggero[1]*

1 UNL, CONICET, FBCB, Centro Biotecnológico del Litoral, Ciudad Universitaria -C.C. 242- (S3000ZAA) Santa Fe, Pcia. Santa Fe, Argentina.

2 IIB-UNSAM, IIBio-CONICET, Laboratorio de Neurobiología Molecular y Celular. Campus Miguelete, San Martín, Buenos Aires, Argentina.

3 UNL, FBCB, Centro Biotecnológico del Litoral, Ciudad Universitaria -C.C. 242- (S3000ZAA) Santa Fe, Pcia. Santa Fe, Argentina.

* Correspondence: Marcos Oggero. UNL, CONICET, FBCB, Centro Biotecnológico del Litoral, Ciudad Universitaria -C.C. 242- (S3000ZAA) Santa Fe, Pcia. Santa Fe, Argentina.

email: moggero@fbcb.unl.edu.ar

Keywords:

Erythropoietin; hEPO-muteins; Glycoengineering; Neuroplasticity; Neuroprotective; Erythropoiesis

Abbreviations:

ATCC: American Type Culture Collection

CEPO: carbamylated EPO

CNS: Central Nervous System

DIV: days in vitro

DMEM: Dulbecco's modified Eagle's medium

DMSZ: German Collection of Microorganisms and Cell Cultures

This article has been accepted for publication and undergone full peer review but has not been through the copyediting, typesetting, pagination and proofreading process, which may lead to differences between this version and the Version of Record. Please cite this article as doi: 10.1002/biot.202000455.

EA: erythropoietic activity

EPO: erythropoietin

hEPO: human erythropoietin

rhEPO: recombinant human erythropoietin

FBS: fetal bovine serum

IAC: Immunoaffinity chromatography

IMDM: Iscove's Modified Dulbecco's Medium

LV: lentiviral particles

rhGM-CSF: recombinant human granulocytes and macrophages colony-stimulating factor

(EPOR)2: homodimeric receptor complex

Mut: mutein

PBS: phosphate-buffered saline

STP: staurosporine

TBS: tris-buffered saline

ABSTRACT

Neurological disorders affect millions of people worldwide causing behavior-cognitive disabilities. Nowadays there is no effective treatment for them. Human erythropoietin (hEPO) has been used in clinical tests because of its neurotrophic and cytoprotective properties. However, the erythropoietic activity (EA) should be considered as a side effect. Some analogs like asialoEPO, carbamylated-EPO or EPO-peptides have been developed showing different weaknesses: erythropoiesis preservation, low stability, potential immunogenicity, or fast clearance.

In this work, we used a novel strategy that blocks the EA but preserves hEPO neurobiological actions. N-glycoengineering was carried out to add a new glycosylation site within the hEPO sequence responsible for its EA. hEPO-derivatives were produced by CHO.K1 cell cultures, affinity-purified and functionally analyzed studying their *in vitro* and *in vivo* EA. Also, we studied the *in vitro* neuronal plasticity in hippocampal neurons and neuroprotective action by rescuing hippocampal neurons from apoptosis.

The muteins: Mut 45_47 (K45 > N45 + N47 > T47), Mut 104 (S104 > N104), and Mut 151_153 (G151 > N151 + K153 > T153) completely lost their EA *in vitro* and *in vivo* but preserved their neuroprotection activity, which enhanced neuroplasticity more efficiently than hEPO. Interestingly, Mut

45_47 resulted in a promising candidate to be explored as a neurotherapeutic considering not only its biopotency but also its pharmacokinetic potential due to the hyperglycosylation.

The novelty of our work was to block the hematopoiesis of the human erythropoietin but preserve or enhance its neuronal plasticity and protection on hippocampal neurons using N-glycoengineering by hyperglycosylation. This procedure added a new glycosyl surrounding to the hematopoietic-responding area of erythropoietin and allowed differentiating both the hematopoietic and the neurologic roles. It is important to emphasize, that it is the first time that N-glycosyl moieties are employed as a leading procedure to simultaneously cancel a biologic action and preserves another into the same molecule. Therefore, the impact of the work lies in the production of new erythropoietin derivatives with therapeutic potential to be used as biopharmaceuticals for the treatment of neurological diseases avoiding the hematopoietic side effects.

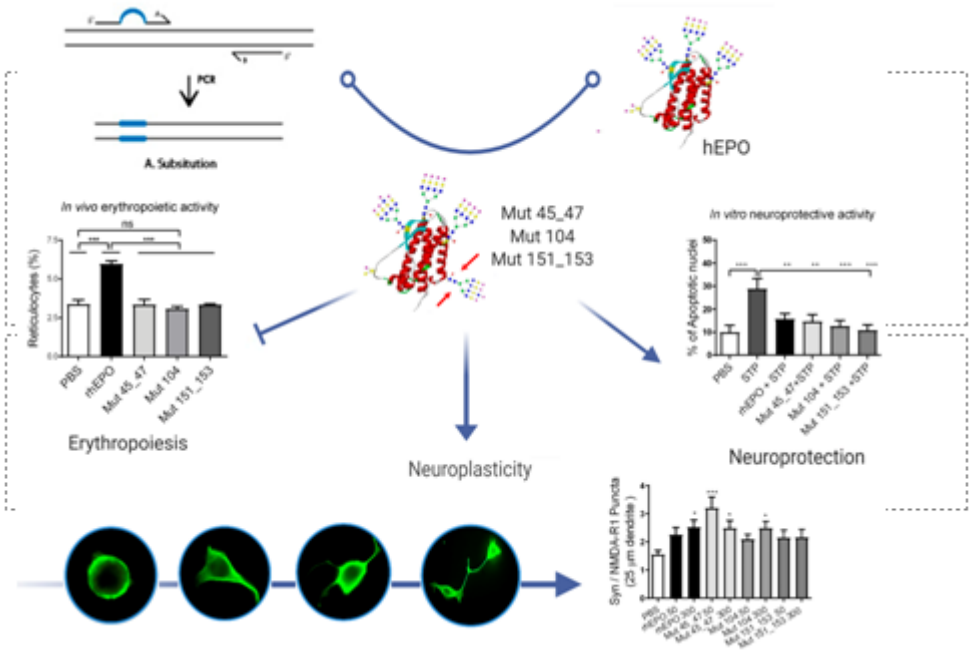

1. INTRODUCTION

Erythropoietin (EPO) is a cytokine that promotes blood cell production [1]. Besides, EPO acts in non-hematopoietic tissues [2]. EPO promotes neuronal survival, proliferation, and migration during CNS development due to the expression of non-hematopoietic EPO receptor by neuron and glial cells [3]. In this sense, EPO administration has shown a worthy competence in the treatment of brain ischemia and neurodegenerative diseases in human and animal models [4–7]. However, chronic EPO administration is associated with side effects such as polyglobulia, hypertension, and prothrombotic phenomena [8].

hEPO is a heavily glycosylated protein consisting of 165 amino acids, and with an average molecular mass (MM) of 30.4-kDa that shows three N-glycosylation sites (N24, N38, and N83) and one O-glycosylation site (S126). The hEPO glycosylation is essential for the *in vivo* hematopoiesis but not for binding to the homodimeric receptor complex, (EPOR)2 [9]. Elliott *et al.* (1997) [10], Cheetham *et al.* (1998) [11] and Brines *et al.* (2008) [12] described two important sites needed for binding and stabilization of (EPOR)2 to promote hematopoiesis. Site 1 represents the high-affinity binding region of hEPO and comprises residues: N147, R150, G151, L155 (helix D) and amino acids 42-51 from A/B loop, whereas site 2 represents the low-affinity binding region of the molecule and comprises residues: V11, R14, Y15, S100, R103, S104, L108. Also, the same authors including Wen *et al.* (1994) [13] and Debeljak (2008) [14] indicated that G151 has the greatest effect on binding to (EPOR)2 and erythropoiesis. On the other hand, the tissue-protective effects of EPO are mediated by the heterodimer EPOR/β-common receptor subunit (CD131). In this regard, Brines *et al*., (2008) [12] described the amino acid sequence 58-82 at helix B as the hEPO tissue-protective domain.

Recombinant human erythropoietin (rhEPO) reached the biopharmaceutic industry as a successful biologic for the treatment of anemia. Based on its neuroplastic activity, EPO derivatives without hematopoietic properties have been developed. Some of them consisted of asialoEPO [15], carbamylated EPO (CEPO) [16,17] or EPO-derived peptides such as ARA29 [18] and NL100 [19]. Even though they demonstrated neurobiological actions, both asialoEPO and EPO-derived peptides have pharmacokinetic restrictions related to their fast clearance. Moreover, CEPO implies high production costs, structural instability and potential immunogenicity [20,21].

Considering that there are unmet medical needs to effectively treat neurological disorders in terms of neuroprotection and neuroplasticity, the development of novel non-erythropoietic hEPO derivatives still represents a leading strategy. Many studies have demonstrated that glycosylation increases the efficiency of protein based-therapeutic drugs [22,23]. In this study, three novel hyperglycosylated hEPO molecules were designed by N-glycoengineering, adding one potential N-glycosylation site in the hematopoietic-responding area. Indeed, the hyperglycosylated hEPO molecules were studied as a procedure that blocks the EA while preserving the neuroplastic response.

2. MATERIALS AND METHODS

2.1 Animals

The animals used for this study were Sprague–Dawley pregnant female rats maintained at the Faculty of Pharmacy and Biochemistry (Universidad de Buenos Aires, Argentina). All animal procedures were carried out according to the guidelines of the National Institutes of Health (issues No. 80-23) and approved by the Committee for the Care and Use of Laboratory Animals of the Universidad de San Martín (CICUAE-UNSAM No. 03/2018), Buenos Aires, Argentina.

2.2. Cell lines and primary cell cultures

Cell lines: CHO.K1 cells (ATCC® CCL-61) were grown and subcultured in DMEM Ham´s F12 medium with 5% (v/v) fetal bovine serum (FBS) and 2 mM glutamine. For hEPO-analogs production, recombinant CHO.K1 cell lines were cultured in basal medium supplemented with 0.5% (v/v) FBS.

HEK 293 T/17 (ATCC® CRL-11268) were cultured in DMEM medium supplemented with 10% (v/v) FBS and 2 mM glutamine.

UT-7 cells (DSMZ, ACC-137) were grown in IMDM with 20% (v/v) FBS and 5 $ng.ml^{-1}$ rhGM-CSF (Leucomax^{TM}). For proliferation assays, cells were cultured in media without rhGM-CSF.

For the neuritogenesis assay, Neuro-2a cells (ATCC® CCL-131) were grown in DMEM medium with 20% (v/v) FBS and 1 $mg.ml^{-1}$ gentamicin.

Hippocampal cultures: Dissociated neuronal cultures were prepared from rat hippocampi of embryonic day 19, as previously described [24]. Briefly, tissues were treated with 0.25% trypsin in Hanks' solution for 15 min at 37ºC. A single-cell solution was prepared in neurobasal medium (NB, Invitrogen) with 200 mM glutamine (Sigma), and 15 $\mu g.ml^{-1}$ gentamicin (Sigma, NB1X) with 10% (v/v) horse serum (Gibco).

Cell lines and neurons were maintained at 37°C and 5% CO_2.

2.3. Erythropoietin, antibodies & reagents

rhEPO was obtained from AMEGA Biotech SA. All chemical reagents and consumables for cell cultures were purchased from Sigma, Invitrogen, Gibco, PAA, Greiner, Promega and Corning. The Sepharose for immunoaffinity chromatography (IAC) was acquired from GE Healthcare. The antibodies and reagents used for neuroplasticity studies were acquired from Sigma, Invitrogen and Calbiochem.

A monoclonal antibody (mAb 2B2-anti rhEPO) and polyclonal antibodies (pAb-anti-hEPO) were employed to purify and analyze the hEPO-derivatives. Both antibodies were previously obtained in our laboratory [25].

For immunocytochemistry, primary antibodies were: mAb anti-alpha-tubulin (1/1000, Sigma), pAb anti-synaptophysin rabbit IgG (1/300, Synaptic System GmbH), mAb anti-N-methyl-D-aspartate mouse IgG (NMDA)-receptor type 1 (R1) (1/500, Synaptic System GmbH). Preabsorbed secondary antibodies were: Alexa 488 goat anti-mouse IgG (1/1000, Invitrogen) and Alexa 568 goat anti-rabbit IgG (1/1000, Invitrogen). Actin filaments were stained with fluorescein isothiocyanate-FICT-conjugated phalloidin (1/1000, Invitrogen) and nucleus were stained with Hoechst 33342 (Sigma). Staurosporine, dimethyl sulfoxide, paraformaldehyde were obtained from Sigma.

2.4. Identification of suitable locations for introducing new N-glycosylation sites

The new hEPO molecules were generated by introducing one extra and potential N-glycosylation site in areas of hEPO involved in the EA and homodimeric receptor binding [10,12,14] using site-directed mutagenesis. The choice of suitable locations for introducing potential N-glycosylation sites was based on bibliography analysis and the available three-dimensional structures of EPO [11,13]. The relative accessibility area (RSA%) was calculated using the algorithm NetSurfP-2.0. NetNGlyc 1.0 Server software was used to predict N-glycosylation efficiency.

2.5. Assembly of hyper-N-glycosylated hEPO-derivatives

hEPO-derivatives were generated by site-directed mutagenesis based on overlap extension PCR. The template was pMAT-EPO. External primers were used in all mutagenesis PCR reactions, while point mutations were present at 26/30-mer internal primers which hybridized with the region where the corresponding substitution was introduced. PCR end products were digested with XbaI and SalI restriction enzymes and cloned in pLV-PLK vector. Plasmid DNA mini-preparations were verified by dideoxy DNA sequencing to confirm the insertional mutations.

2.6. Gene expression in mammalian cells

Lentiviral particles for each hEPO-derivatives were assembled to transduce CHO.K1 cells. HEK 293 T/17 packaging cells were co-transfected with 4 vectors: pMDLg/pRRE, pMDG, pRSV-Rev, and the

transfer vector (pLV-PLK-Mut X) by lipofection. After 48 h, supernatants containing Mut X lentiviral particles (LV Mut X) were harvested. For cell line generation, CHO.K1 cells were seeded at 3×10^4 cells.ml^{-1} in 6-well plates and incubated for 24 h. The supernatant was removed, and cells were transduced by adding 1 ml of fresh lentivirus. After 96 h, the transduced cells were trypsinized, seeded at 3×10^4 cells.ml^{-1} in 6-well plates and transduced twice to increase the level of protein expression. After 96 h from the last transduction, the cells were incubated with increasing quantities of puromycin (10 to 350 µg.ml^{-1}) to isolate the recombinant cells showing the highest protein expression. The recombinant protein expression was monitored using a sandwich ELISA [25]. For large-scale production, cells were seeded in a 500 cm^2 triple flask in the growth medium. Once the monolayer reached confluence, the growth medium was replaced by the production medium. The hEPO muteins-containing supernatants were collected and replaced by production medium every 48 hours. The conditioned supernatants were clarified and stored at -20°C. A total of eight harvests were collected for each mutein.

2.7. Purification of hEPO-derivatives by IAC

The CNBr-activated Sepharose-4B was coupled with the mAb 2B2 previously purified by protein-A affinity chromatography from the hybridoma´s culture supernatant. The IAC-2B2 resin was prepared according to the manufacturer's protocol (GE Healthcare). This mAb is useful to purify all the hEPO-derivatives given that it binds to a common region of a peptide area of rhEPO molecule or hEPO muteins. As this region is distant from the glycosylation sites, the immobilized mAb can capture the complete set of glycoforms. Clarified supernatants from each hEPO-mutein were conditioned with Triton X-100 0.3% (v/v), pH 7.5 and applied to the immunosorbent equilibrated with Triton X-100 0.3% (v/v) in Tris/HCl 25 mM pH 7.5. Then, three sequential 5-bed volume washes were carried out with the following solutions: (1) - Triton X-100 0.2% (v/v), NaCl 0.5 M, Tris/HCl 25 mM pH 7.5; (2) - Triton X-100 0.1% (v/v), NaSCN 1 M, Tris/HCl 25 mM pH 7.5; (3) - NaCl 0.15 M, acetic acid/sodium acetate 25 mM pH 5. Elution was accomplished using Glycine/HCl 0.1 M, pH 2.5 for muteins Mut104 and Mut151_153, and acetic acid/sodium acetate 0.1 M pH 3 for mutein Mut45_47 and neutralized with This/HCl 1 M pH 8. Purified muteins were concentrated and diafiltrated against phosphate-buffered saline (PBS). The IAC recovery was determined by quantifying the mutein concentration in each

chromatography step. The purity was analyzed by SDS-PAGE under reducing conditions followed by Coomassie blue staining.

2.8. Sandwich ELISA to quantify hEPO muteins

hEPO muteins concentrations were determined by a sandwich ELISA described by Amadeo et al. (2004) [25]. Briefly, 96-well plates were coated overnight at 4°C with 100 ng per well of mAb 2B2 in 50 mM carbonate-bicarbonate buffer (pH 9.6). After blocking 1 h at 37°C with 2% (w/v) milk in PBS, plates were incubated with 1/2 serial dilutions of rhEPO standard solutions from 2 $\mu g.ml^{-1}$ to 0.016 $\mu g.ml^{-1}$ or 1/2 serial dilutions of test samples for 1 h at 37°C. Later, plates were incubated with the appropriate dilution of rabbit anti-rhEPO polyclonal antibodies for 1 h at 37 °C. Then, peroxidase (HRP)-labelled goat anti-rabbit immunoglobulins (DAKO, USA) were added at a dilution of 1/2000. After 1 h, plates were incubated with substrate solution (0.5 mg.ml-1 o-phenylenediamine (Sigma, USA), 0.015% (v/v) H_2O_2 in 50 mM phosphate-citrate buffer). The colorimetric reaction was stopped by adding 2 N. H_2SO_4,and the absorbance was measured at 492 nm with a microtiter plate reader (Labsystems Multiskan MCC/340, Finland). Between every step, plates were washed with PBS containing 0.05% (v/v) Tween 20. Dilutions were prepared in PBS-Tween containing 0.2% (w/v) milk.

2.9. SDS-PAGE and Western blot

Muteins were electrophoretically analyzed using 12% (w/v) polyacrylamide resolving gels and 5% (w/v) stacking gels following the standard procedure. Samples were diluted in reducing buffer containing 5% (v/v) beta-mercaptoethanol (J.T. Baker). The separation was performed at 200 V for 60 min. For purity determination, gels were stained with Coomassie blue and destained with 15% (v/v) methanol and 10% (v/v) acetic acid solution. For molecular mass (MM) determination, proteins were transferred to a PVDF membrane (BioRad) at 180 mA for 60 min and then blocked with 5% (w/v) milk in Tris saline buffer (TBS) and 0.1% (v/v) Tween 20. Later, membranes were incubated with pAb anti-rhEPO. Anti-rabbit Igs-HRP (1/2000, DAKO) was employed as a secondary antibody. Finally, the immunoreactive bands were visualized by ECL Pierce™ substrate (Thermo Fisher).

2.10. Isoelectric focusing (IEF)

IEF was performed in 1-mm thick gel containing 8% (w/v) acrylamide and 7 M urea. In order to establish the pH range, 67% (w/v) 2.5–5 ampholytes and 33% (w/v) 5–7 ampholytes were mixed. Before sample's application, the gel was pre-focused (10 W, 2000 V, 100 mA, 1 h). Then, 12 µl of each sample was applied at 1 cm from cathode, and electrophoresis was carried out for 40 min under the same pre-focusing conditions. The gel was stained with a Coomasie blue colloidal solution and washed with deionized water.

2.11. N-glycosylation site occupancy analysis

A denaturing protocol to remove N-glycans was performed by following the manfacturer's procedure (New England Biolabs, UK). Partial N-deglycosylation was carried out using 18 µg of rhEPO or muteins in 18 µl PBS, combined with 2 µl of denaturating buffer. This solution was heated at 100°C for 10 min. Then, a volume equivalent to 10 µg of proteins was dispensed into a new tube and 2 µl of Glycobuffer, 2 µl of 10% (v/v) NP-40, 7.5 units of PNGase F and water were added to make a total volume reaction of 20 µl. A time course inhibition was carried out at 1, 3, 30 min and ON. At each time, samples were inhibited by freezing at -20°C. Later, they were analyzed by SDS-PAGE using 15% (W/V) polyacrylamide resolving gels and 5% (w/v) stacking gels following the standard procedure above described.

2.12. Biological characterization

2.12.1. *In vitro* hematopoietic activity

UT-7 cells, whose proliferation depends on hEPO [26], were washed thrice using basal medium. Then, cells were incubated in assay medium at 37°C, 5% CO2. After 3 h, cells were seeded at 1 x 10^4 cells.well^{-1} in 96-well plates. Serial 1/2 rhEPO and hEPO-muteins dilutions from 8.4 ng.ml^{-1} to 0.066 ng.ml^{-1} were added to each well. After 72 h, cell proliferation was analyzed using a CellTiter 96^{TM} (Promega). Absorbance was read at 492 and 620 nm (as background) using a microplate reader. Cells incubated with rhEPO at 50 ng.ml^{-1} were included as a positive control, and cells without the addition of rhEPO or muteins as negative controls. The assay was reproduced in triplicates.

2.12.2. *In vivo* hematopoietic activity

The *in vivo* hematopoietic activity of rhEPO and muteins was measured as their ability to induce reticulocyte production in normocythemic mice according to the European Pharmacopoeia [27].The assay was carried out by the Molecular Biology Platform of the Institut Pasteur of Montevideo (Uruguay) using B6D2 F1 mice (~23 g/animal). The animals were subcutaneously injected with 0.5 ml of 80, 40, and 20 IU.ml^{-1} of rhEPO or with the muteins at a mass concentration of 672 ng.ml^{-1}, which corresponds to the maximum amount of injected rhEPO (80 IU.ml^{-1}). Blood samples were collected 96 h later, and the percentage of reticulocytes was determined by flow cytometry after fluorometric staining. Negative control was included by injecting a group of mice with PBS.

2.12.3. Cultured hippocampal neurons assays

Hippocampal neurons were seeded on coverslips with 0.1 mg.ml^{-1} poly-L-lysine hydrobromide (Sigma) and 20 mg.ml^{-1} laminin (Invitrogen). After 2 h, the culture medium was changed to NB/N2 (NB1X with 1 g.l^{-1} ovalbumin; N2 and B27 serum-free supplements from Invitrogen). Neurons were cultured for 5 or 15 days in vitro (DIV) depending on the neuroplastic process to be evaluated. Based on the morphological characteristics, we estimated that more than 90% of the cultured cells were neurons. Moreover, neurons are composed of a majority of excitatory pyramidal cells and a small portion of GABAergic interneurons (approximately 6 % of cells in culture) [28] . Culture media was refreshed every week by changing half of the volume in the well.

For filopodia density and synapses assays, neurons were cultured at a density of 30,000 for 5 days *in vitro* (DIV) or 7,000 cells for 15 DIV per well in a 24-well plate, respectively. Cells were exposed to 50 ng.ml^{-1} and 300 ng.ml^{-1} of rhEPO / muteins / PBS for the entire experiment. For the neuroprotection assay, 50,000 neurons were seeded per well. At 11 DIV neurons were exposed to the protein kinase inhibitor staurosporine (30 ng.ml^{-1}) for 24 h in the presence of 400 ng.ml^{-1} of rhEPO or muteins or PBS.

For neuritogenesis, 25,000 N2a cells were seeded on coverslips in 24-well plates. In order to induce differentiation, on the day after N2a cells were serum-starved and exposed to different concentrations of rhEPO / muteins / PBS for 3 h [24]. Then, cells were subjected to immunocytochemistry.

2.12.4 Immunocytochemistry

For quantification of neurite extension or filopodia protrusions, cells were fixed in 4% (w/v) paraformaldehyde and 4% (w/v) sucrose in PBS at 4°C for 10 min and permeabilized with 0.1% (v/v) Triton X-100 in PBS for 5 min. Permeabilized cells were blocked with 3% (w/v) bovine serum albumin (BSA) in PBS for 1 h followed by incubation with primary antibodies (anti-tub) in 3% BSA for 16 h at 4°C and with secondary antibodies (Alexa 488 goat anti-mouse) for 1 h at 25°C. F-actin was stained with phalloidin-FICT for 1 h at 25°C. For the neuroprotection assay, cells were stained with Hoechst 33342 for 10 min. Coverslips were mounted in FluorSave reagent (Calbiochem). Images were acquired with a 60X objective on a Nikon E2000 microscope equipped with epifluorescence illumination (Nikon).

To evaluate neuritogenesis in N2a cells, the number of neurites per cell, the longest neurite and the average of total neurites length per cell were quantified with the NeuronJ plugin (version 1.4.2) of ImageJ (FIJI, NIH) (https://imagej.net/ImageJ, NIH).

Filopodia density was quantified as the number of protrusions stained with phalloidin per 20 μm of neurite length measured within 50 μm from the soma in 30–60 dendrites per group.

To evaluate the neuroprotective action of rhEPO and its muteins, the percentage of apoptotic cells (the ones bearing nuclear condensation or nuclear pyknosis) was quantified. An inverse correlation is established between neuroprotection and apoptotic cells.

Synapses were quantified as previously described [29]. Neurons at 15 DIV were methanol fixed 90:10 v/v methanol/MES (100 mM buffer MES pH 6.9, 1 mM EGTA, 1 mM $MgCl_2$) for 5 min at 4ºC and washed with PBS-Tween 0.1% (v/v) for 5 min. Then, cells were blocked with FBS-Triton X-100 (FBS 10% (v/v) and PBS-BSA 3% (w/v)) for 30 min each at 25°C. Primary antibodies (anti-NMDA-R1 and anti-syn) were diluted in PBS-BSA 1% (w/v) solution and incubated at 4ºC ON. The day after, washed cells were blocked again followed by incubation with Alexa 488 anti-mouse and Alexa 568 anti-rabbit IgG. Coverslips were mounted in Fluorsave®. Fluorescence images were acquired with a confocal microscope Olympus FV1000 attached to an inverted microscope Olympus IX81. FluoView software (version 3.3, Olympus) was used to acquire sequential images with a 60 X objective with a NA 1.42. The pixel size of the images was 1600 × 1600, following the Nyquist criterion. The number of synapses was measured by colocalization of puncta, in 25 μm of dendrite length, between pre-synaptic marker (syn) and post-synaptic marker (NMDA-R1) in approximately 15 neurons per condition. The selected neurons were at least two cell diameters away from their nearest neighbor. All

experiments were carried out under blind conditions to the examiner. The colocalization of puncta was determined using the plugin Puncta Analyzer from Image J (NIH). Briefly, 3 regions of interest (25 µm of dendrite length) from each neuron were selected, and then the background was subtracted. The threshold was adjusted manually for each channel. The minimum puncta size was set to 4 pixels. At least 2 independent experiments were performed. Images were processed in Adobe Photoshop (version 8.0.1; Adobe Systems).

2.13. Statistical analyses

Calculations were performed with GraphPad Prism 5.0 and data are expressed as mean + SEM. One-way ANOVA and Two-way ANOVA were used followed by Bonferroni's post hoc test and referred to in the legend of each figure. The results were considered significant when $p<0.05$.

3. RESULTS

3.1. Strategy to prepare non-hematopoietic hyperglycosylated hEPO-derivatives preserving neurobiological functions

A glycoengineering strategy was used to generate one potential N-glycosylation site in those regions of hEPO molecule responsible for the EA (those that bind (EPOR)2) without modifying the neurobiological-associated domains of the cytokine. The following criteria were considered:

1- To modify residues that affect the hematopoietic activity and their binding to the (EPOR)2.
2- To preserve residues involved in tissue-protective action of hEPO.
3- To conserve amino acids critical for protein folding.
4- To consider the modification of some lysine residues because they take part of the carbamylation reaction in CEPO and are responsible for hEPO's lack of hematopoiesis but preservation of its tissue-protective action [30].

Thus, we selected one representative amino acid from each of the two sites that hEPO needs for (EPOR)2 binding (Fig. 1A). So, G151 has been described as the most relevant residue at site 1 for the EA because of its structural role in homodimeric receptor binding. S104 was selected as representative of site 2 which is involved in binding a second EPOR subunit forming the (EPOR)2 complex. Also, Gan *et al.*, (2012) [31] reliably demonstrated that mutating S104 by isoleucine completely inhibited the EA but preserved the neuroprotective action. Finally, K45 was selected as

another representative amino acid of site 1 considering that it is also one of the carbamylated residues in CEPO. In a previous report, it was determined that a replacement of K45 by aspartic acid [10], but not by alanine [13], dramatically reduced the hematopoietic activity. This different behavior supports our idea that decorating this position with glycans could disrupt the interaction of the homodimeric receptor with the site 1 of hEPO, not only as a result of the bulky glycans structures but also due to the negative charge of the sialic acid that cap each antenna. Moreover, neither G151 nor S104 and K45 are folding-sensitive residues, therefore it could be assumed that their modification will not affect the mutants´ structures.

To generate the consensus site for N-glycosylation (N-X-T/S), each selected amino acid was changed by N and the position +2 from this residue was scanned within the hEPO sequence to detect the presence of threonine or serine. Considering the three amino acids selected to be modified by asparagine (K45, S104 and G151), only a T106 was found to prepare the N-glycosylation consensus sequence: N104LT106. Therefore, S104 was replaced by N104 (Mut 104). For the remaining muteins, the following changes were carried out: K45 > N45 + N47 > T47 (Mut 45_47) and G151 > N151 + K153 > T153 (Mut 151_153). In all cases, threonine was selected as amino acid at position +2 from the asparagine-mutated residue, because the efficiency of N-glycan occupancy is higher than using serine located at the same position.

3.2. N-glycosylation probability analysis of hEPO-derivatives

After selecting the relevant amino acid positions to be mutated, an *in silico* study was carried out to predict a successful N-glycan expression.

The N-glycosylation probability was calculated by NetNGlyc 1.0 Server software (https://services.healthtech.dtu.dk/) which demonstrated that predicted values were higher than the threshold (0.5). These values were 0.61 for Mut 45_47 and 0.63 for both Mut 104 and Mut 151_153, indicating a high probability of N-glycosylation.

To introduce mutations without significant distortion of the tertiary structure or the receptor-binding area of the protein, the identification of residues located on the surface of the hEPO was performed. The relative surface accessibility (RSA%) analysis allowed us to avoid selecting buried residues that, in case of being glycosylated, could affect the molecule's conformation. The RSA% was calculated by the algorithm NetSurfP-2.0 (https://services.healthtech.dtu.dk/service.php?NetSurfP-2.0). These

resulted in values of 72% for Mut 45_47, 48% for Mut 104, and 36% for Mut 151_153. These values, higher than a 25%-threshold, were highly indicative of adequate solvent accessibility to expose the glycans superficially.

3.3. Muteins production and purification

Mut hEPO-producing CHO.K1 cell lines were selected with puromycin, reaching concentrations of 350 $\mu g.ml^{-1}$ (Mut 45_47 and Mut 104) and 150 $\mu g.ml^{-1}$ (Mut 151_153). After cell lines culture and culture harvesting, CHO.K1 Mut 45_47 and CHO.K1 Mut 104 showed similar production but higher than those obtained for CHO.K1 Mut 151_153 (12.6 ± 1.8 $\mu g.ml^{-1}$ and 14.2 ± 2.2 $\mu g.ml^{-1}$ vs 3.5 ± 1.0 $\mu g.ml^{-1}$, respectively).

The mutein-containing supernatants were purified by IAC using mAb 2B2 as ligand because of its ability to bind all muteins. Thus, all hEPO-analogs were captured by the IAC and recovered in a proportion of 50-64% after elution. The purity of the eluted muteins was higher than 89% in only one purification step, in which case BSA was the main contaminant (Supporting information Fig. S1).

3.4. Molecular mass and glycoform characterization

The apparent MM of purified muteins was analyzed by Western blot (Fig. 1B). Thus, their lower and upper MM range and their average were determined: Mut 45_47: range 32-63 kDa, average 47 kDa; Mut 104: range 30-59 kDa, average 45 kDa, and Mut 151-153: range 32-59 kDa, average 46 kDa. The MM range for rhEPO was 32-44 kDa with an average of 38 kDa. The muteins demonstrated molecular masses from 7 to 9 kDa higher than rhEPO.

To assess the degree of heterogeneity of the hEPO-derivatives due to glycosylation, the isoform distribution was analyzed by IEF. Fig. 1C shows a representative gel of the isoelectric pattern of commercial rhEPO and hEPO variants. A total of 18 isoforms for Mut 45_47, 16 isoforms for Mut 104, 14 isoforms for Mut 151_153, and 6 isoforms for rhEPO were observed. It is important to consider that glycoforms from hEPO variants are the total set produced and purified from the cell cultures (a maximum of 18 glycoforms having from 1 to 18 sialic acid was expected) while the 6 isoforms from rhEPO correspond to the more acidic isoforms (having from 9 to 14 sialic acids) that were purified by the industry to be pharmaceutically used for anemia treatment. All muteins demonstrated more acidic isoforms than rhEPO. Particularly, Mut 45_47 presented 6 more lower-pI isoforms while Mut 104 and

Mut 151_153 showed 4 and 3 more, respectively. The higher number of acidic glycoforms can be explained by the occurrence of additional oligosaccharides.

To confirm that the higher molecular masses of muteins and the higher number of acidic glycoforms were due to the occupancy of a fourth potential N-glycosylation site, partial N-deglycosylation assays using PNGase F were carried out. After SDS-PAGE, 3 bands for rhEPO or 4 bands for each mutein were observed above the completely N-deglycosylated molecules (indicated as 0N-linked), confirming the oligosaccharide occupancy of the newly added N-glycosylation sites (Fig. 2).

3.5. Hematopoietic activity

3.5.1. *In vitro* erythropoietic activity

Mut 104 and Mut 151_153 completely lost their *in vitro* EA measured as the ability to stimulate the UT-7 cells growth (Fig. 3A), i.e., no proliferation responses were obtained despite the fact that we used higher or equal mutein concentrations with respect to rhEPO. Nevertheless, Mut 45_47 showed a slightly proliferative response. To quantify this response, the specific erythropoietic activity (SEA = IU/µg) was calculated, resulting in a value of 0.2 IU/µg. Considering the *in vitro* SEA of rhEPO (120 IU/µg), Mut 45_47 retained only 0.2% or lost the 99.8% of it. To evaluate if the remaining 0.2% of the EA from Mut 45_47 is sufficient to elicit the *in vivo* hematopoietic activity, the following analysis was carried out.

3.5.2. *In vivo* erythropoietic activity

In vivo erythropoiesis was evaluated as the capacity of rhEPO or the muteins to stimulate the maturation of hematopoietic progenitors to reticulocytes. As long as Mut 104 and Mut 151_153 demonstrated no *in vitro* EA and Mut 45_47 retained a very low SEA proportion with respect to rhEPO, the three molecules and rhEPO were evaluated at a concentration of 80 $IU.ml^{-1}$ = 672 $ng.ml^{-1}$. Fig. 3B demonstrates that none of the 3 muteins were capable of stimulating reticulocytes in mice, presenting the same response than the negative control. Contrarily, rhEPO promoted reticulocytes proliferation in the same sense as it was expected according to the European Pharmacopoeia [32].

3.6. Neuroplastic and neuroprotective effect of the hEPO variants

Structural plasticity during neuronal development involves neurite extension, axonal polarization, dendritic arborization, and synapse formation. In this regard, previous reports determined that EPO exhibits neuroprotective properties and enhances neuroplasticity in both, *in vitro* and *in vivo* studies [33,34].

3.6.1. hEPO-derivatives enhance neuritogenesis

N2a cells were exposed to 50 ng.ml^{-1} and 300 ng.ml^{-1} of rhEPO or each mutant for 3 h under serum-free condition (Fig. 4A). We quantified the neuritogenesis as the number and length of neurites (the longest neurite and the average of neurite extension) per each condition. rhEPO treated cells showed a dose-dependent increase in neuritogenesis compared to control cells. Moreover, Mut 45_47-, Mut 104-, or Mut 151_153-treated cells exhibited an induction of neurite extension and number compared to PBS-treated cells (Fig. 4B-D and Supporting Fig. S2). Notably, in all hEPO-derivatives, 50 ng.ml^{-1} was enough to induce the maximum of neuritogenesis, meaning that no significant differences were observed between cells treated with 50 ng.ml^{-1} or 300 ng.ml^{-1}. Moreover, the lower dose of each rhEPO-derivate, 50 ng.ml^{-1}, proved to be more effective to promote neurite extension than rhEPO at 50 ng.ml^{-1}. Altogether, the three new hyper-N-glycosylated hEPO-derivatives conserved hEPO neuronal differentiation properties.

3.6.2. hEPO-derivatives induce filopodia formation

To assess filopodia formation, hippocampal cultured neurons were exposed to 50 ng.ml^{-1} and 300 ng.ml^{-1} of each mutein for 5 DIV (Fig. 5A). We quantified the average number of filopodia in 20 µm of neurite length of treated neurons. Hippocampal neurons treated with hEPO variants at 300 ng.ml^{-1} showed a significantly higher number of filopodia per cell than the control group (PBS) (Fig. 5B-D). Similar results were obtained for neurons treated with rhEPO. Interestingly, neurons treated with 50 ng.ml^{-1} of Mut 45_47 or Mut 151_153 significantly induced filopodia formation compared to cells treated with PBS or 50 ng.ml^{-1} of rhEPO. These results demonstrate that the three rhEPO derivatives induce hippocampal plasticity and might be more efficient than rhEPO.

3.6.3. Mut 45_47 and Mut 104 enhance synapses formation

Synapse formation was quantified as points of colocalization between synaptophysin puncta (presynaptic marker) and NMDA-R1 puncta (postsynaptic marker) in hippocampal neurons exposed to 50 ng.ml^{-1} or 300 ng-ml^{-1} of rhEPO or each mutein for 15 DIV. Fig. 6 shows images of 25 µm of a dendrite segment from controls and muteins-treated neurons. The merged images show the output obtained from the Puncta Analyzer plugin as black squares (asterisk and magnified in the insets)[35]. Neurons treated with Mut 45_47 (at both concentrations) showed a significantly higher number of synapses compared to the control group (Fig. 6B and 6F). Neurons treated with 300 ng.ml^{-1} of Mut 104 enhanced synapses formation compared to the control group (Fig. 6G). Although neurons treated either with rhEPO or Mut 151_153 showed an increase in the number of synapses, none of the concentrations were statistically significant (Fig. 6D and 6H). These results demonstrate that two of the hEPO derivatives induce synapses more competently than rhEPO.

3.6.4. hEPO-derivatives prevent STP-induce neuronal apoptosis

EPO prevents apoptotic death or promotes neuronal survival in different models of brain injuries such as ischemia and traumatism [34,36,37]. In hippocampal cultured neurons, 24 hours of STP treatment induces apoptosis [38]. During STP exposure, cell nucleus becomes smaller, brighter, and/or fractionated (arrows and asterisks, Fig. 7A). Thus, neurons at 11 DIV were exposed to 30 nM of STP in the presence of 400 ng.ml^{-1} of rhEPO or each mutein or PBS, and the percent of apoptotic cells was quantified. STP-treated neurons showed a significant increase in the percent of apoptotic cells compared to the control group (Fig. 7B). However, the presence of rhEPO or muteins in the neuronal media rescued the STP-apoptotic induction. These data suggest that the three new hyper-N-glycosylated hEPO-derivatives conserved its neuroprotective features.

4. DISCUSSION AND CONCLUSION

Erythropoietin is a versatile cytokine due to its erythropoietic and tissue protection and restoration functions. However, its hematopoietic effects must be taken into account when hEPO is considered as a biotherapeutic to be chronically administered for neurodegenerative diseases. Therefore, we developed three novel hyperglycosylated hEPO-analogues (Mut 45_47, Mut 104 and Mut 151_153) that hindered their hematopoietic activity but preserved the neuroprotective and neuroplastic functions as rhEPO.

The glycoengineering by hyperglycosylation of hEPO represents a useful strategy to generate analogs where the newly introduced glycan could block a non-desired feature and preserve an expected function. For instance, introducing two N-glycosylation sites into hEPO to produce darbepoietin alpha (Aranesp®) prolonged its half-life and enhanced its EA compared with rhEPO [9].

Here, we introduced a new N-glycosylation site into hEPO at specific amino acids critical for its hematopoietic activity (K45N, S104N, or G151N). The muteins augmented their MM and the number of acidic glycoforms because of their sialic acid content. Sialylation may produce more negatively charged molecules with a higher hydrodynamic radius. Both features are interesting physicochemical properties that would decrease the molecular clearance or augment the half-life of the hyper-N-glycosylated muteins in blood [39,40].

Erbayraktar *et al.* (2003) [41] and Mattio *et al.* (2011) [42] produced hEPO-derived variants such as asialoEPO and neuropoetin with neurobiological actions and lower EA. In these studies, the high clearance due to the lower sialic acid content in the molecule [30,42] reduced the interaction with (EPOR)2, which is responsible for the lower hematopoiesis *in vivo*. However, the higher the clearance, the higher the doses to produce the neurobiological actions, and therefore the greater the hematopoiesis and its side effects.

Unlike other hEPO derivatives for neurobiological purposes (eg. Neuropoetin, asialoEPO, and carbamylated EPO), the new hyperglycosylated EPO derivatives have improved PK properties (data not shown), and they are easier to be produced because no chemical procedures, such as deglycosylation or carbamylation, have to be performed. Also, they will have better stability as a result of the hyperglycosylation that confers higher solubility, higher protection from protease, and also lower immunogenicity [22].

The neurobiological activities of the three muteins were studied by assessing neuritogenesis, filopodia density, and synapses formation. We also carried out an analysis of neuronal rescue from STP-apoptotic induction. The three muteins preserved their neuroprotective activity as rhEPO. Furthermore, they enhanced neuritogenesis and induced filopodia formation more efficiently than rhEPO. Accordingly, retinal ganglion cells treated with rhEPO for 72 h show a neurite outgrowth in a dose-dependent manner [43]. Moreover, retinal neurocytes exposed to 6 UI of EPO (equivalent to 50 $ng.ml^{-1}$) for 48 h increase neurite elongation and prevent the cytotoxic effect of glutamate (10 mM) added to culture media [44]. Besides, hippocampal neurons treated with 10 $ng.ml^{-1}$ of rhEPO or CEPO

were enough to induce filopodia/spine formation and to enhance the levels of synaptic proteins (synapsin 1 and PSD95) [45]. In our hands, 50 ng.ml^{-1} of hEPO-derivatives were needed to induce filopodia and synapses formation. By contrast, no induction of synaptogenesis in rhEPO-treated neurons was found and this could be due to differences in experimental conditions and methods. Hence, many non-exclusive scenarios could justify the lower or lack of effect of rhEPO on neuroplasticity compared to hEPO-derivates: i) rhEPO can bind to both types of hEPO receptors at neurons surface compared to hEPO-muteins which would only bind the heterodimeric form of the receptor, being more efficient for plastic effect [46]; ii) hEPO-muteins showed higher effectiveness to promote both synaptic compartments than rhEPO (filopodia as dendrite spine precursor and neurite extension as axon precursor); iii) hEPO-muteins could be more stable and/or have a longer half-life in culture media than rhEPO[47]. Recently, Wakhloo et al. (2020) [7] demonstrated that acute intraperitoneal (ip) administration of rhEPO in mice stimulates dendritic spine formation and promotes neurogenesis in the hippocampal CA1 region. Moreover, chronic ip rhEPO treatment enhances motor learning and endurance that could be linked with the increment of 20% of new pyramidal neurons. Altogether, in vivo studies in naïve animals and/or disease models are necessary to confirm the neuroplastic contribution of the muteins over the rhEPO.

Leist *et al.* (2004) [30] and Gan *et al.* (2012) [31] demonstrated that mutants such as EPO-S100E, EPO-R103E or EPOS104I retained a high cytoprotective efficacy despite drastically reduced (EPOR)2 affinity. Accordingly, we corroborated the importance of modifying certain amino acids of the EPO/(EPOR)2 binding site 2. Thus, the incorporation of a novel glycosylation site at the amino acid positions 104-106 (i.e., generating the mutation S104N) was useful to decorate with glycans and block the hematopoiesis, while it conserves the neuroprotective and neuroplastic actions. Interestingly, the novel glycosylation site at positions 45_47 completely blocked the hematopoiesis and demonstrated to be more effective to enhance neuroplasticity in hippocampal neurons compared to Mut 104. Altogether, our findings validate our hypothesis and were supported by the *in vitro* model. However, *in vivo* studies are required for a complete evaluation of the three hEPO muteins.

With respect to the *in vivo* evaluation, it is important to consider the Blood Brain Barrier (BBB). The success of the muteins to cross the BBB is based on at least two facts. The first one is related to the ability of hEPO to cross the BBB [46] and the feature that each mutein is a mixture of isoforms that have a different N-glycosylation site occupancy. Partial N-deglycosylation experiments (Fig 2) showed

that muteins include isoforms that have from 2 to 4 N-glycosylation sites, and those isoforms share a mean of 3 occupied sites, the predominant group. In the case of rhEPO, the molecule demonstrated mainly all N-glycosylation sites occupied (3 sites). As the muteins have no *in vivo* hematopoietic action it is probable that isoforms are mainly occupied by the newly added N-glycosylation sites (that are responsible for blocking the EA). With this in mind, we expect the new muteins (having a mean of 3 occupied N-glycosylation sites) could also cross the BBB and exert their neurological action.

The second antecedent is related to the use of Aranesp® as a neuroprotectant. This molecule is extensively used to treat anemia associated with chronic renal insufficiency and chemotherapy. Moreover Aranesp® crosses the BBB [48] and showed neuroprotective activity, but the increment of hematopoiesis became a sensitive factor to reject it as a neurotherapeutic [49–51]. Aranesp® has two extra N-glycosylation sites compared to rhEPO, with a possible maximum number of 22 isoforms [47,52]. Therefore, we estimate that Mut 45_47 or Mut 104 or Mut 151_153 would pass the BBB since they only have one extra N-glycosylation site compared to rhEPO reaching a maximum number of 18 isoforms. Nonetheless, a no minor issue for the future will be the consideration that a more selective chromatography procedure should be carried out to select a suitable set of isoforms that could fulfill the criteria of a defined, robust and stable product as potential biopharmaceutic.

In conclusion, the use of glycoengineering by hyper-N-glycosylation was a proper procedure to differentiate the hEPO activities by blocking the hematopoietic action while preserving its neurobiological function. In particular, Mut 45_47 represents a promising candidate to be explored as biotherapeutics for neurological diseases considering not only its biological function but also its pharmacokinetic potential.

Acknowledgments

This work was supported by the following Argentine institutions: Universidad Nacional del Litoral (CAI+D 2016_50020150100024LI; Capital Semilla 8-1-2018-UNL), and Agencia Nacional de Promoción de la Investigación, el Desarrollo Tecnológico y la Innovación (PICT 2015-2150 to M.O and PICT 2016-1223 to C.S).

Conflict of interest:

the authors report that a patent application No. AR-20180102793 was filed with the National Institute of Intellectual Property (INPI, Buenos Aires, Argentina) and also an application PCT/IB2019/058179 was filed with the International Bureau of the World Intellectual Property Organization (WIPO).

References

[1] C. Lacombe, P. Mayeux, *Nephrol Dial Transplant*. **1999**, *14 Suppl 2*, 22.

[2] J.W. Fisher, *Exp Biol Med*. **2010**, *12*, 1398.

[3] A. Nekoui, G. Blaise, *Am J Med Sci*. **2017**, *353*, 76.

[4] F. Simon, N. Floros, W. Ibing, H. Schelzig, A. Knapsis, *Neural Regen Res*. **2019**, *14*, 1309.

[5] H.N. Hong, J.H. Shim, Y.J. Won, J.Y. Yoo, C.H. Hwang, *Med (United States)*. **2018**, *97*, e9913.

[6] I. Ercan, K.U. Tufekci, E. Karaca, S. Genc, Peptide Derivatives of Erythropoietin in the Treatment of Neuroinflammation and Neurodegeneration, 1st ed., Elsevier Inc., 2018.

[7] D. Wakhloo, F. Scharkowski, Y. Curto, U. Javed Butt, V. Bansal, A.A. Steixner-Kumar, L. Wüstefeld, A. Rajput, S. Arinrad, M.R. Zillmann, A. Seelbach, I. Hassouna, K. Schneider, A. Qadir Ibrahim, H.B. Werner, H. Martens, K. Miskowiak, S.M. Wojcik, S. Bonn, J. Nacher, K.-A. Nave, H. Ehrenreich, *Nat Commun*. **2020**, *11*, 1313.

[8] S. Suresh, P.K. Rajvanshi, C.T. Noguchi, *Front Physiol*. **2020**, *10*, 1534.

[9] J.C. Egrie, J.K. Browne, *Br J Cancer*. **2001**, *84*, 3.

[10] S. Elliott, T. Lorenzini, D. Chang, J. Barzilay, E. Delorme, *Blood*. **1997**, *89*, 493.

[11] J.C. Cheetham, D.M. Smith, K.H. Aoki, J.L. Stevenson, T.J. Hoeffel, R.S. Syed, J. Egrie, T.S. Harvey, *Nat Struct Biol*. **1998**, *5*, 861.

[12] M. Brines, N.S. Patel, P. Villa, C. Brines, T. Mennini, M. De Paola, Z. Erbayraktar, S. Erbayraktar, B. Sepodes, C. Thiemermann, P. Ghezzi, M. Yamin, C.C. Hand, Q.W. Xie, T. Coleman, A. Cerami, *Proc Natl Acad Sci U S A*. **2008**, *105*, 10925.

[13] D. Wen, J.P. Boissel, M. Showers, B.C. Ruch, H.F. Bunn, *J Biol Chem*. **1994**, *269*, 22839.

[14] N. Debeljak, A.J. Sytkowski, *Curr Pharm Des*. **2008**, *14*, 1302.

[15] T. Yamashita, N. Nonoguchi, T. Ikemoto, S.I. Miyatake, T. Kuroiwa, *Neurol Res*. **2010**, *32*, 957.

[16] M. Diao, Y. Qu, H. Liu, Y. Ma, X. Lin, *Biol Res*. **2019**, *52*, 28.

[17] J. Chen, Z. Yang, X. Zhang, *Biochem Insights*. **2015**, *8s1*, BCI.S30753.

[18] D.A. Culver, A. Dahan, D. Bajorunas, M. Jeziorska, M. van Velzen, L.P.H.J. Aarts, J. Tavee, M.R. Tannemaat, A.N. Dunne, R.I. Kirk, I.N. Petropoulos, A. Cerami, R.A. Malik, M. Brines, *Investig Ophthalmol Vis Sci*. **2017**, *58*, BIO52.

[19] O. Dmytriyeva, A. Belmeguenai, L. Bezin, K. Soud, D.P. Drucker Woldbye, C.R. Gøtzsche, S. Pankratova, *Neurobiol Aging*. **2019**, *81*, 88.

[20] M. Brines, *Mol Med*. **2014**, *20*, S10.

[21] B. Peng, G. Kong, C. Yang, Y. Ming, *Cell Death Dis*. **2020**, *11*, 1.

[22] K.A.I. Griebenow, R.J. Sola, **2009**, *98*, 1223.

[23] S. Elliott, T. Lorenzini, S. Asher, K. Aoki, D. Brankow, L. Buck, L. Busse, D. Chang, J. Fuller, J. Grant, N. Hernday, M. Hokum, S. Hu, A. Knudten, N. Levin, R. Komorowski, F. Martin, R. Navarro, T. Osslund, G. Rogers, N. Rogers, G. Trail, J. Egrie, *Nat Biotechnol*. **2003**, *21*, 414.

[24] K. Formoso, S.C. Billi, A.C. Frasch, C. Scorticati, *J Neurosci Res*. **2015**, *93*, 215.

[25] I. Amadeo, M. Oggero, M.L. Zenclussen, L. Robles, D. Pereira, R. Kratje, M. Etcheverrigaray, *J Immunol Methods*. **2004**, *293*, 191.

[26] T. Kitamura, T. Tange, T. Terasawa, S. Chiba, T. Kuwaki, K. Miyagawa, Y. -F Piao, K. Miyazono, A. Urabe, F. Takaku, *J Cell Physiol*. **1989**, *140*, 323.

[27] European Pharmacopoeia Biological Reference Preparation (Ph. Eur. BRP), Strasbourg, France, 2005.

[28] D.L. Benson, F.H. Watkins, O. Steward, G. Banker, *J Neurocytol*. **1994**, *23*, 279.

[29] K. Formoso, M.D. Garcia, A.C. Frasch, C. Scorticati, *Mol Cell Neurosci*. **2016**, *77*, 95.

[30] M. Leist, P. Ghezzi, G. Grasso, R. Bianchi, P. Villa, M. Fratelli, C. Savino, M. Bianchi, J. Nielsen, J. Gerwien, P. Kallunki, A.K. Larsen, L. Helboe, S. Christensen, L.O. Pedersen, M. Nielsen, L. Torup, T. Sager, A. Sfacteria, S. Erbayraktar, Z. Erbayraktar, N. Gokmen, O. Yilmaz, C. Cerami-Hand, Q.W. Xie, T. Coleman, A. Cerami, M. Brines, *Science (80-)*. **2004**, *305*, 239.

[31] Y. Gan, J. Xing, Z. Jing, R. Anne Stetler, F. Zhang, Y. Luo, X. Ji, Y. Gao, G. Cao, *Stroke*. **2012**, *43*, 3071.

[32] European Pharmacopoeia Biological Reference Preparation (Ph. Eur. BRP), Strasbourg, France, 2005.

[33] L. Jantzie, N. El Demerdash, J.C. Newville, S. Robinson, *Exp Neurol*. **2019**, *318*, 205.

[34] B. Viviani, S. Bartesaghi, E. Corsini, P. Villa, P. Ghezzi, A. Garau, C.L. Galli, M. Marinovich, *J Neurochem*. **2005**, *93*, 412.

[35] D.M. Ippolito, C. Eroglu, *J Vis Exp*. **2010**, *16*, 2270.

[36] L.S. Schmidt, J.Z. Petersen, M. Vinberg, I. Hageman, N.V. Olsen, L.V. Kessing, M.B. Jørgensen, K.W. Miskowiak, *Trials*. **2018**, *19*, 234.

[37] C. Zhong, X. Zhang, *Mol Med Rep*. **2017**, *15*, 228.

[38] A.J. Krohn, E. Preis, J.H.M. Prehn, *J Neurosci*. **1998**, *18*, 8186.

[39] R.E. Kontermann, *Expert Opin Biol Ther*. **2016**, *16*, 903.

[40] A. Gugliotta, N. Ceaglio, R. Kratje, M. Oggero, *J Biotechnol*. **2019**, *303*, 46.

[41] S. Erbayraktar, G. Grasso, A. Sfacteria, Q. wen Xie, T. Coleman, M. Kreilgaard, L. Torup, T. Sager, Z. Erbayraktar, N. Gokmen, O. Yilmaz, P. Ghezzi, P. Villa, M. Fratelli, S. Casagrande, M. Leist, L. Helboe, J. Gerwein, S. Christensen, M.A. Geist, L.Ø. Pedersen, C. Cerami-Hand, J.P. Wuerth, A. Cerami, M. Brines, *Proc Natl Acad Sci U S A*. **2003**, *100*, 6741.

[42] M. Mattio, N. Ceaglio, M. Oggero, N. Perotti, I. Amadeo, G. Orozco, G. Forno, R. Kratje, M. Etcheverrigaray, *Biotechnol Prog*. **2011**, *27*, 1018.

[43] S. Böcker-Meffert, P. Rosenstiel, C. Röhl, N. Warneke, J. Held-Feindt, J. Sievers, R. Lucius, *Investig Ophthalmol Vis Sci*. **2002**, *43*, 2021. https://pubmed.ncbi.nlm.nih.gov/12037014/ (accessed November 13, 2020).

[44] Y. Zhong, H. Yao, L. Deng, Y. Cheng, X. Zhou, *Graefe's Arch Clin Exp Ophthalmol*. **2007**, *245*, 1859.

[45] M. Choi, S.Y. Ko, I.Y. Lee, S.E. Wang, S.H. Lee, D.H. Oh, Y.S. Kim, H. Son, *Biochem Biophys Res Commun*. **2014**, *446*, 79.

[46] M.L. Brines, P. Ghezzi, S. Keenan, D. Agnello, N.C. De Lanerolle, C. Cerami, L.M. Itri, A. Cerami, *Proc Natl Acad Sci U S A*. **2000**, *97*, 10526.

[47] J.C. Egrie, E. Dwyer, J.K. Browne, A. Hitz, M.A. Lykos, *Exp Hematol*. **2003**, *31*, 290.

[48] W.A. Banks, N.L. Jumbe, C.L. Farrell, M.L. Niehoff, A.C. Heatherington, **2004**, *505*, 93.

[49] S.E. Hori, K.J. Powell, G.S. Robertson, *Neuroscience*. **2007**, *144*, 1.

[50] G. Grasso, F. Graziano, A. Sfacteria, F. Carletti, F. Meli, R. Maugeri, M. Passalacqua, F. Certo, M. Fazio, M. Buemi, D.G. Iacopino, *Neurosurgery*. **2009**, *65*, 763.

[51] S. Patel, R.K. Ohls, *Clin Perinatol*. **2015**, *42*, 557.

[52] J. Powell, C. Gurk-Turner, *Baylor Univ Med Cent Proc*. **2002**, *15*, 332.

Figures:

Figure 1

Fig. 1: N-glycoengineering of hEPO: from the selected sites to the hyperglycosylation results

A) Graphical representation of hEPO interaction with the homodimeric receptor (EPOR)2. The rope diagram of the crystallized interaction hEPO-(EPOR)2 was obtained from the SWISS-MODEL Repository (https://biasmv.github.io/pv/). K45, S104, and G151 are the amino acid residues that were modified by asparagine to generate the motif N-X-T as a potential glycosylation site. To this effect, threonine was inserted in position +2 from asparagine as needed. Thus, the muteins K45N + N47T, S104N, and G151N + L153T were developed by site-directed mutagenesis. K45 and G151 are the residues involved in the high-affinity binding site (site 1), while S104 is part of the low-affinity binding site (site 2) of (EPOR)2. EPOR indicates each subunit of the homodimeric receptor (EPOR)2. **B)** Western blot using an anti-hEPO antibody to determine the apparent MM of rhEPO and hEPO muteins. MM: Molecular mass marker. **C)** IEF profiles of rhEPO, Mut 45_47, Mut 104 and Mut 151_153 purified by IAC. pI: isoelectric point. pI indicates the pH range employed.

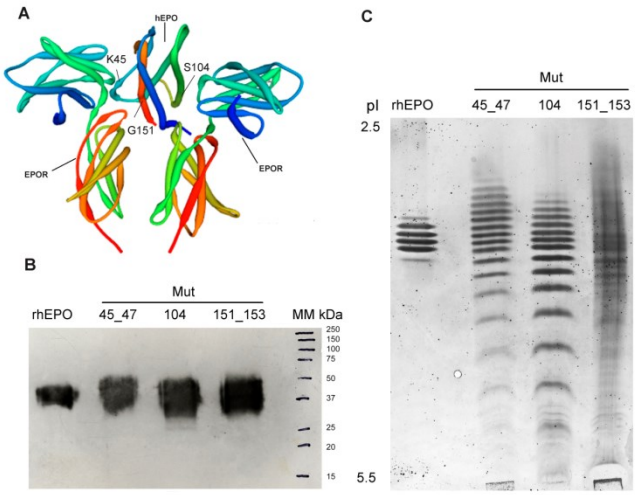

Figure 2

Fig. 2: *N-glycosylation site occupancy analysis*

The number of N-glycosylated sites was studied for rhEPO and the muteins after treatment with PNGase F at different incubation times: 0, 1, 3, 30 min, and ON. The occupancy degree was analyzed by SDS-PAGE followed by Coomassie blue stain. On the right of the gels, 0N, 1N, 2N, 3N, and 4N represent the number of N-linked glycosylation sites remaining after the partial deglycosylation procedure. On the left of each gel, the molecular masses were also included.

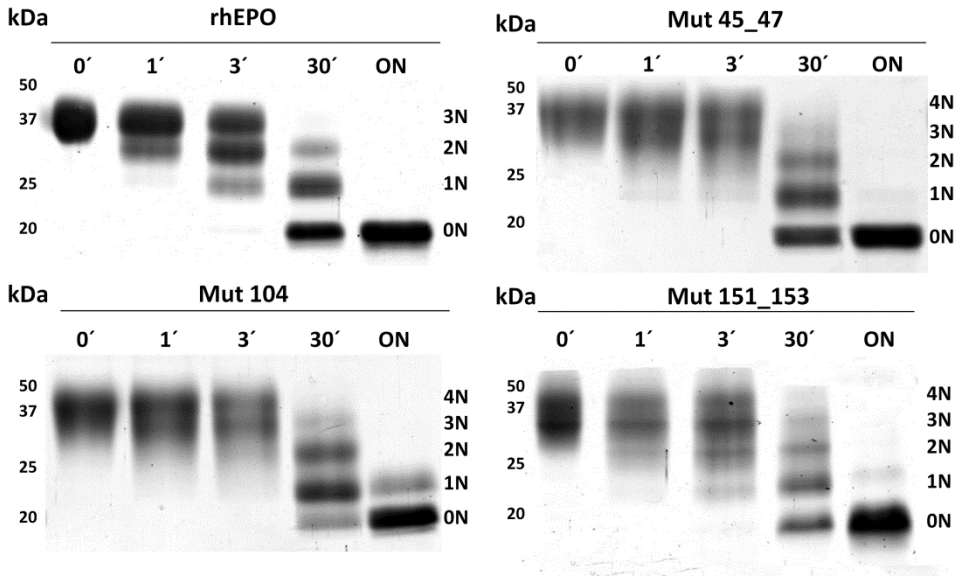

Figure 3

Fig. 3: *In vitro* and *in vivo* erythropoietic activity of hEPO-derivatives

A) Determination of the *in vitro* erythropoietic biological activity for hEPO muteins using the UT-7 cell line. **B)** Evaluation of *in vivo* erythropoietic activity for hEPO muteins in normocytemic mice (n=4). ****p ≤ 0.001 and ns (not significant) represent the degree of statistical significance after one-way ANOVA test, followed by Bonferoni´s post hoc test (n=4).

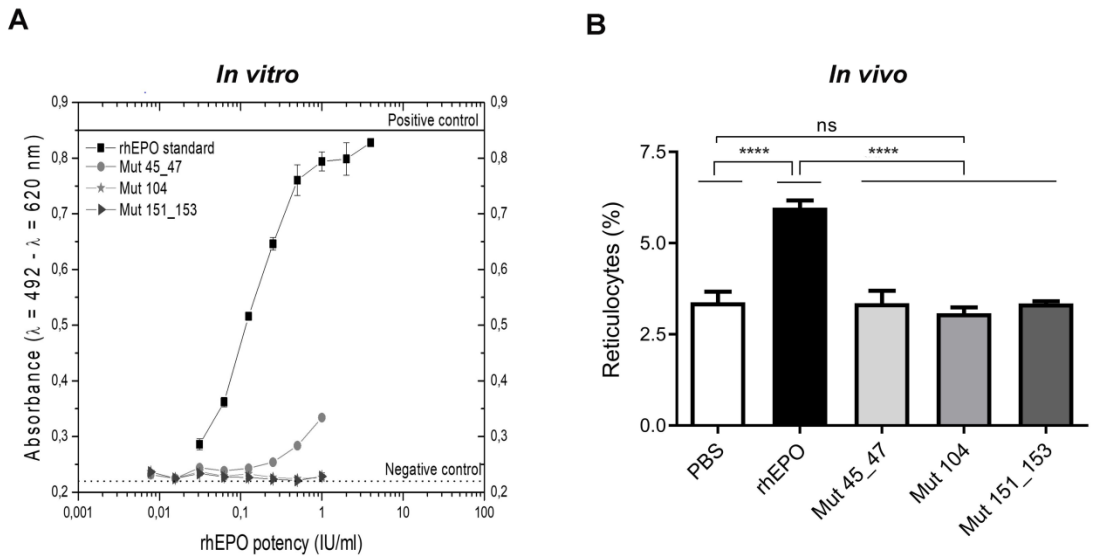

Figure 4

Fig. 4: rhEPO derivatives induce neuritogenesis in N2a cells

A) Representative inverted images of serum deprived-N2a cells treated with 50 ng.mL^{-1} or 300 ng.mL^{-1} of rhEPO or Mut 45_47, Mut 104, Mut 151_153 or PBS (as control) for 3 h. Scale bar: 20 µm. **B-D)** The longest neurite per cell was quantified using the NeuronJ plugin for ImageJ software. Results are expressed as mean + SEM of at least n = 20-25 cells per condition of three independent experiments analyzed. Significant differences between control condition, PBS, and rhEPO or its derivatives were determined with two-way ANOVA, followed by Bonferroni's post hoc test. *p<0.05, **p<0.005, *** p <0.001 and ****p<0.0001.

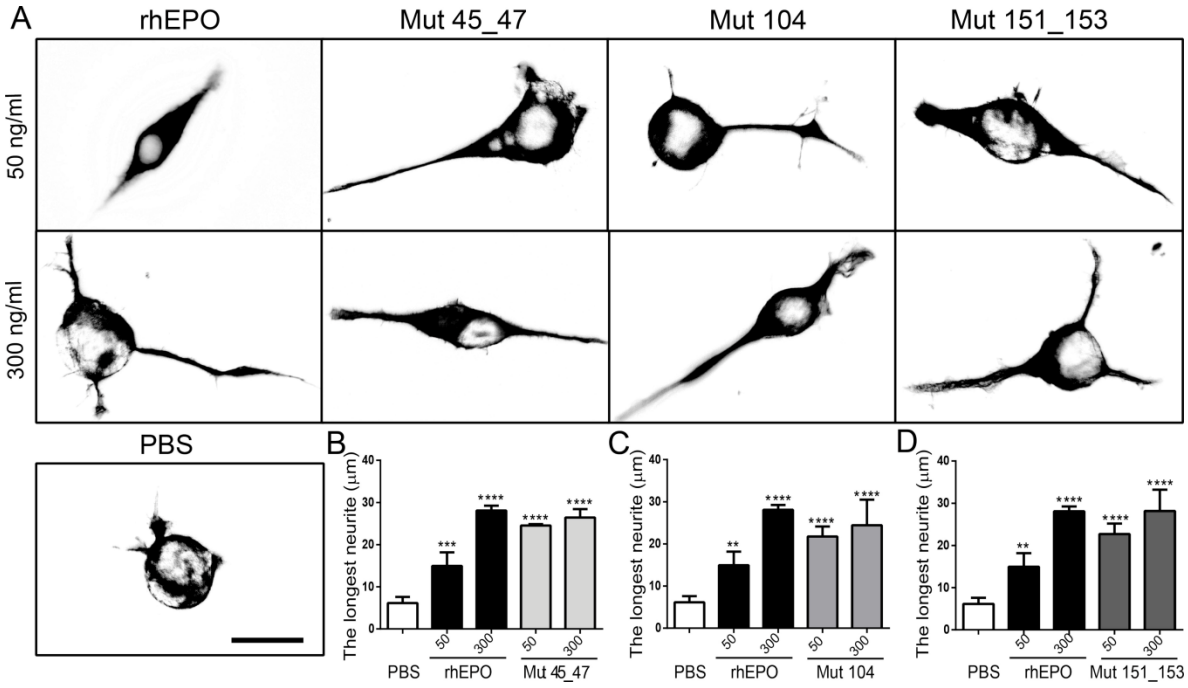

Figure 5

Fig. 5: rhEPO and its derivatives promote filopodia formation in hippocampal neurons

A) Representative inverted images and their magnifications of hippocampal cultured neurons at 5 DIV treated with 50 ng.mL^{-1} or 300 ng.mL^{-1} of rhEPO or Mut 45_47, Mut 104, Mut 151_153 or PBS (as control). Scale bar: 20 µm and 5 µm for the magnifications. **B-D)** The number of processes in 20 µm of neurite length was quantified. Two independent experiments were analyzed. Results are expressed as mean + SEM of n = 25-30 cells per condition. Significant differences between control condition, PBS, and rhEPO or rhEPO derivatives were determined with one-way ANOVA, followed by Bonferroni's post hoc test. *p < 0.05, ***p<0.001 and ****p < 0.0001.

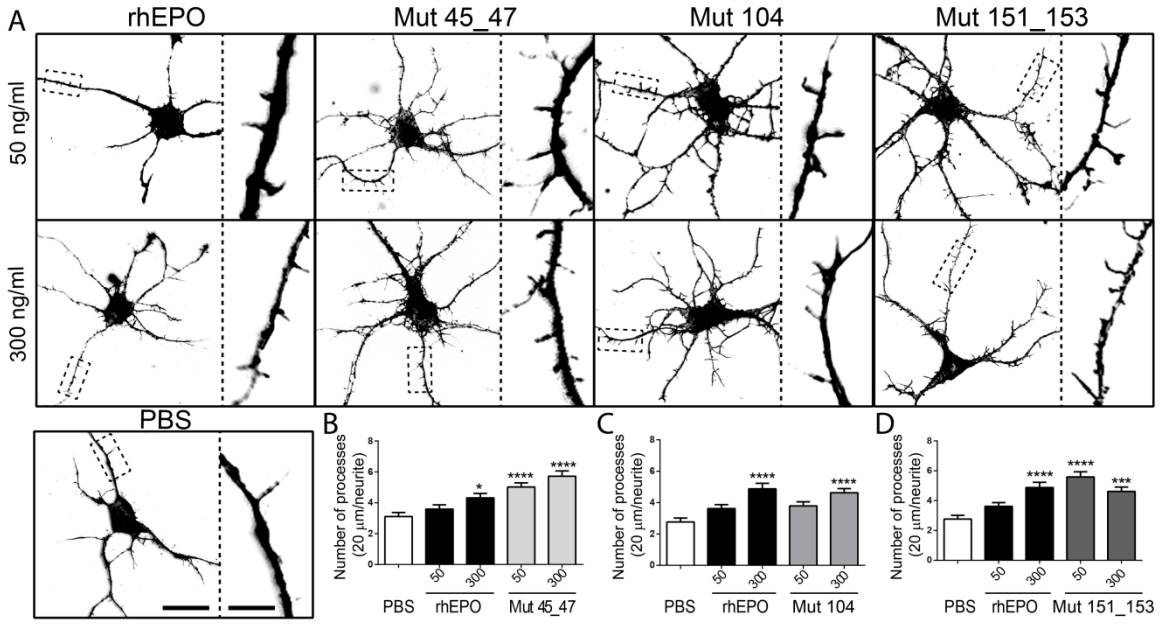

Figura 6

Fig. 6: Mut 45_47 and Mut 104 but not Mut 151_153 enhance synapse formation in hippocampal cultured neurons

Hippocampal neurons treated with 50 ng.mL^{-1} **(A)** or 300 ng.mL^{-1} **(E)** of rhEPO or Mut 45_47, Mut 104, Mut 151_153 or PBS (as control) for 15 days. Images show 25 µm of dendrite length of a representative neuron, labeled with the presynaptic marker synaptophysin (Syn, red) and the postsynaptic marker NMDA-R1 (green). In the merge images, white asterisks and the insets represent detectable colocalization of Syn/NMDA-R1 (yellow). Scale bar: 5 µm. **B-D; F-H)** The number of synapses per condition was quantified as points of colocalization between Syn/NMDA-R1 puncta in 25 µm of dendrite length by Puncta Analyzer plugin of ImageJ software. Two independent experiments were analyzed. Results are expressed as mean + SEM of at least n = 15 neurons (three segments per neuron) per condition. Significant differences between control condition, PBS, and rhEPO or hEPO derivates were determined with one-way ANOVA, followed by Bonferroni's post hoc test. *p <0.05.

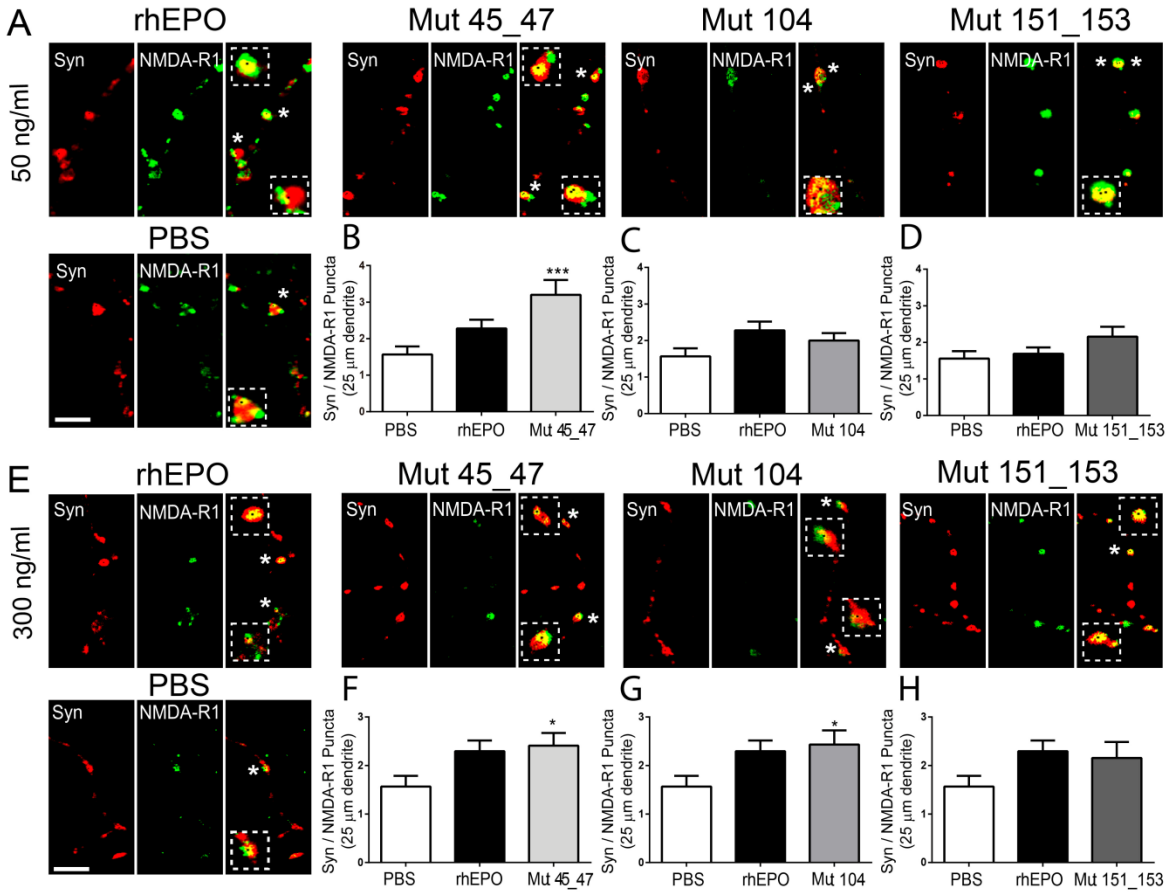

Figure 7

Fig. 7: hEPO muteins prevent STP-induced apoptosis in neurons

A) Representative images of hippocampal cultured neurons at 11 DIV treated with 30 nM of staurosporine (STP) in the presence or not of 400 ng.mL^{-1} of rhEPO or Mut 45_47, Mut 104 or Mut 151_153. PBS and STP alone were used as control conditions. Apoptotic nuclei are indicated with white arrows (smaller and brighter nuclei) and asterisks (fractionated nuclei). Scale bar: 20 µm. **B)** The percent of apoptotic cells was quantified as the number of apoptotic cells over the total amount of cells in a field. Results are expressed as mean+ SEM of n = 25 - 30 fields per condition. Significant differences between STP condition and rhEPO or rhEPO derivatives were determined with one-way ANOVA, followed by Bonferroni's post hoc test. * $p < 0.05$, ** $p < 0.01$, *** $p < 0.0001$, # $p < 0.001$ PBS vs STP.